

## ARTICLES

# Implications for Timing of Andean Uplift from Thermal Resetting of Radiation-Damaged Zircon in the Cordillera Huayhuash, Northern Peru

*J. I. Garver, P. W. Reiners,<sup>1</sup> L. J. Walker, J. M. Ramage,<sup>2</sup> and S. E. Perry<sup>3</sup>*

*Geology Department, Union College, Schenectady, New York 12308, U.S.A.  
(e-mail: garverj@union.edu)*

### ABSTRACT

The Cordillera Huayhuash is a north-south-oriented range along the drainage divide of the northern Peruvian Andes. The range has high topography with peaks in excess of 5500 m and the second-highest peak in Peru, Nevados Yerupaja (6617 m). Bedrock is dominated by folded Mesozoic miogeoclinal rocks unconformably overlain by mid-Tertiary volcanics intruded by Late Tertiary granitic rocks and silicic dikes. Zircon fission track (ZFT) and (U-Th)/He (ZHe) dating of zircons along a west-east transect elucidates the thermal evolution of exhumed and uplifted rocks. The stability of fission tracks in zircons is a function of single-grain radiation damage. In samples with grain-to-grain variability in radiation damage, resetting results in variable resetting and multiple age populations. Low retentive zircons (LRZs), which have a partly disordered crystalline structure, have significant radiation damage and a low temperature of annealing (ca. 180°–200°C). High retentive zircons (HRZs), which are nearly crystalline, fully anneal at temperatures in excess of ca. 280°–300°C. Partly reset samples are those where LRZs are reset and HRZs are not reset, and therefore the cooling age is not concordant, but the young population of grain ages records the youngest thermal event. Full resetting of both LRZs and HRZs results in cooling ages that are concordant or nearly so. Lower Cretaceous quartzites show ZFT ages with a wide range of cooling ages, but most have LRZ reset ages at ca. 27 and 63 Ma. The ZFT ages from three quartzites and two granites from the core of the range yielded a single mean reset age of  $11.4 \pm 1$  Ma. The ZHe ages from four samples in these rocks ranged from 10 to 7 Ma, with older ages away from the high topography. Together, the ZFT and ZHe cooling ages near the core of the range indicate moderate to rapid postintrusive cooling in the Miocene and a high Miocene geothermal gradient (ca. 40°–50°C/km). This widespread cooling age represents a falling geotherm, not a period of significant exhumation. Estimations of the thickness of preexhumation cover rock suggest that nearly 5 km of unroofing has occurred since the eruption of the Puscanturpa Formation (Huayllay Formation) at ca. 6.2 Ma. Exhumation was driven by valley incision initiated by uplift of this part of the Andes between 5 and 6 Ma. The high topography may have been formed by isostatic response to canyon incision. Therefore, the thermochronologic record of uplift and canyon incision is not yet apparent in the low-temperature thermochronology (for zircons) of these rocks.

### Introduction

The Andean mountain chain has attained present elevations of 3000–4000 m along much of the

length of South America (fig. 1), despite significant along-strike changes in subduction angle and deformation history. The Andes formed during the relatively continuous subduction of the Nazca and Farallon plates beneath the South American plate since the Mesozoic (Allmendinger et al. 1997). The timing of orogenic development varies along strike, but the majority of uplift is generally viewed as being Miocene to Plio-Pleistocene. The Altiplano plateau, characterized by mean elevations of ca. 4000 m and internal drainage, dominates the main

Manuscript received May 20, 2004; accepted November 17, 2004.

<sup>1</sup> Department of Geology and Geophysics, P.O. Box 208109, Yale University, New Haven, Connecticut 06520-8109, U.S.A.

<sup>2</sup> Department of Earth and Environmental Sciences, 31 Williams Hall, Lehigh University, Bethlehem, Pennsylvania 18015, U.S.A.

<sup>3</sup> Current address: Department of Earth and Atmospheric Sciences, State University of New York, Albany, New York 12222, U.S.A.

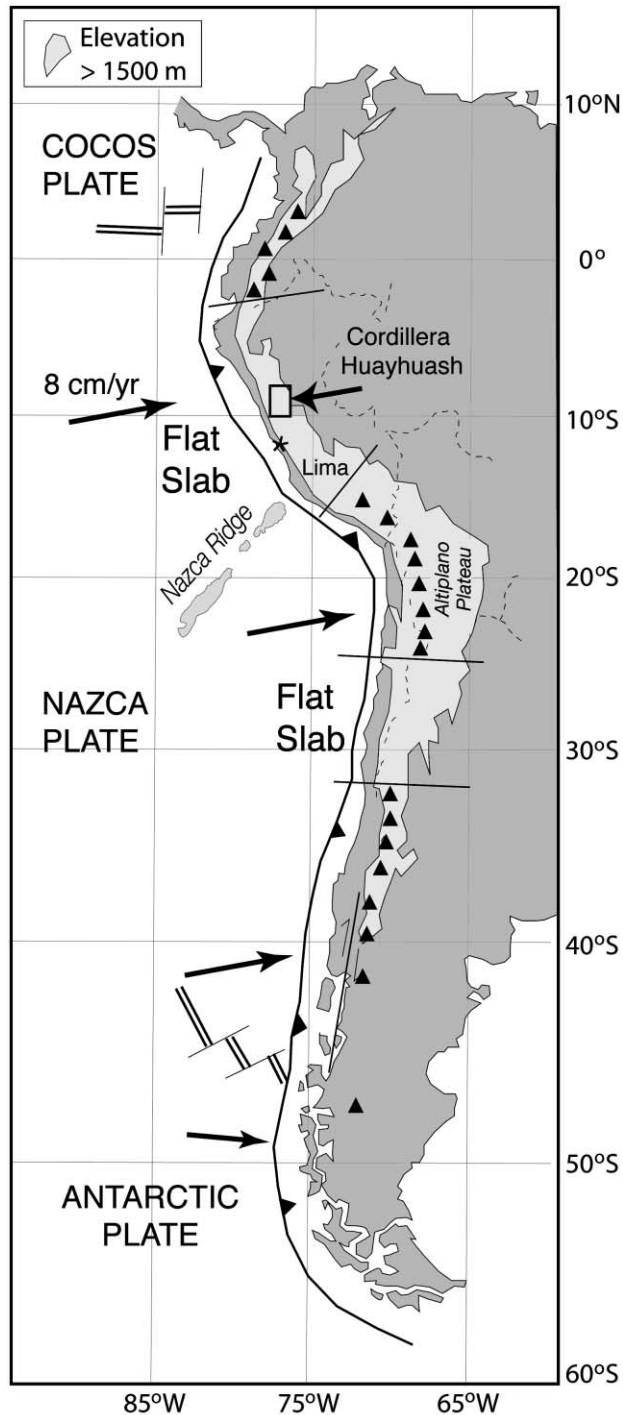


**Figure 1.** Location of the Cordillera Huayhuash, northern Peru, in the Andes (after Kennan 2000; Lamb and Davis 2003). Solid triangles represent active volcanoes, and the light shading represents the Andean chain with elevations greater than 1500 m.

part of the central Andes. Both east- and west-flanking areas are uplifted and recently incised by rivers draining perpendicular to orogenic strike. Both the northern and southern end of the Altiplano plateau are imprecisely defined because there is no clear topographic or geologic break between the plateau and the Andean chain to the north or south. In both cases, the range narrows, becomes more dissected, and has more relief (e.g., Montgomery et al. 2001). In fact, the northern transition, the focus of this article, is marked by a distinctly different hypsometric curve inferred to represent topography dominated by fluvial and glacial erosion (figs. 2, 3) as opposed to the concave-down profile of the Altiplano plateau inferred to represent an uplifted plateau with little active erosion.

The northern Peruvian Andes, north of about 10°S, lie in this northern transition zone. Here, the 150–200-km-wide range can be divided into the Cordillera Oriental and the Cordillera Occidental, which are separated by deeply incised valleys (fig. 2). This area is marked by several areas of tremendous relief and summit elevations well above the mean elevation of much of the rest of the chain (i.e., fig. 3). High relief is distinct in the Cordillera Oriental and is locally characterized by the Cordillera Blanca and the Cordillera Huayhuash, which have the highest (Huscaran Norte [6655 m] and Huscaran Sud [6768 m]) and second-highest (Nevado Yerupaja [6634 m]) massifs in Peru. These peaks straddle the crest of the Andes and define the drainage divide between the headwaters of the Amazon and smaller Pacific-draining rivers. These ranges represent the largest glaciated region in equatorial South America, and therefore glacial erosion rates are likely to be high compared with adjacent areas.

A number of terms relevant to this discussion of mountain building need to be defined because they have varied use in the literature. Surface uplift is the change in mean elevation of Earth's surface relative to sea level, and rock uplift is the vertical movement of rocks with respect to sea level (Molnar and England 1990). Exhumation is the removal of overlying rocks and the upward movement of a rock with respect to Earth's surface (England and Molnar 1990). Exhumation can be driven by erosion or tectonic mechanisms, mainly normal faulting (Ring et al. 1999). The timing and rate of exhumation can be constrained by thermochronology (cooling ages), assuming geothermal gradients are known. Note that in many orogenic belts, surface uplift has occurred without significant exhumation (Molnar and England 1990); the Altiplano and the Tibetan plateaus are notable examples.

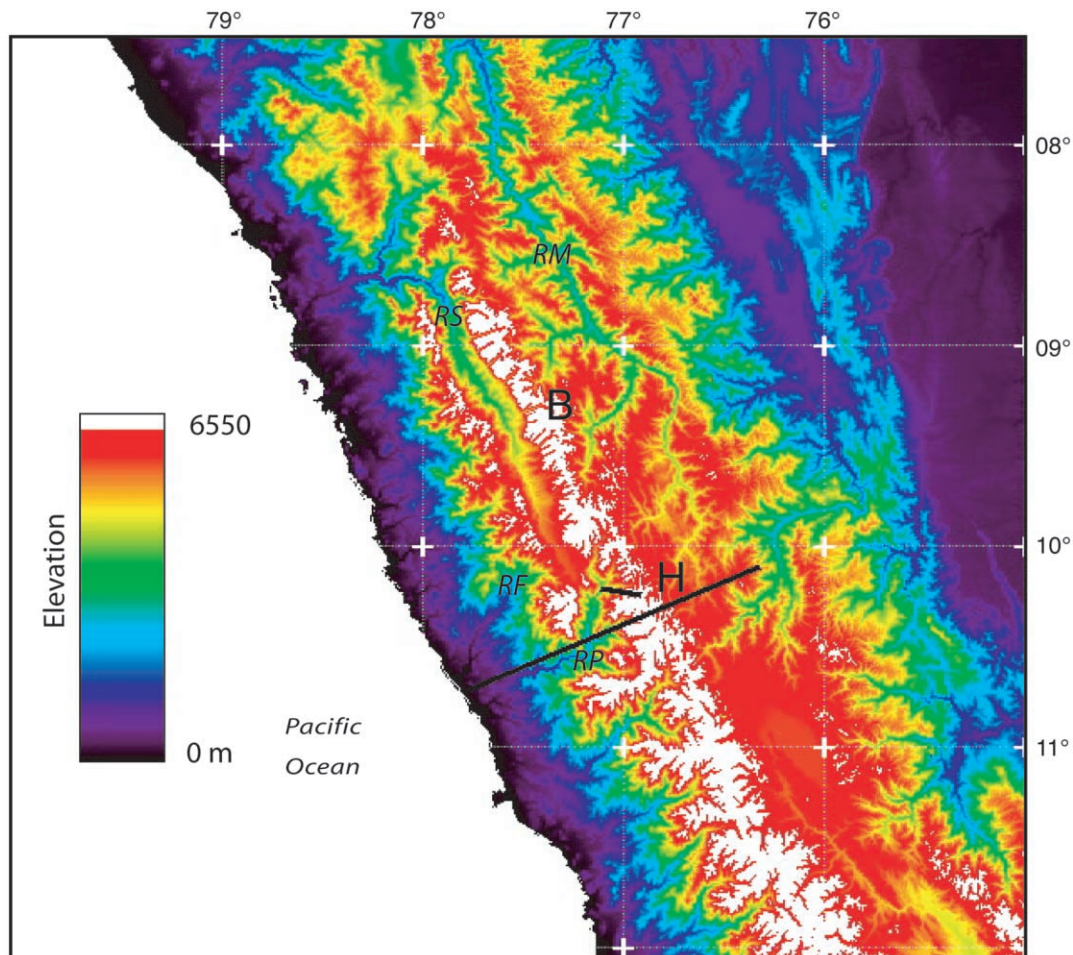


**Figure 2.** Digital elevation model (DEM) of the study area showing the relationship between the high topography along the crest of the Andes in the Cordillera Blanca (*B*) and the Cordillera Huayhuash (*H*). The elevation scale is linear so that 3000 m is green on the map. The short line is the location of the fission track transect, which originates in the upper part of the Rio Pativilca (*RP*) and continues to the crest of the Huayhuash. The long transect is the line of the topographic swath in figure 3. Also marked are the Rio Santa (*RS*), which drains much of the western Cordillera Blanca, and the Rio Marañon (*RM*), which is a major tributary of the Amazon and drains the eastern slopes of the Cordillera Blanca and the Huayhuash. *RF* = Rio Fortaleza. Data for this DEM come from the Shuttle Radar Topography Mission (SRTM) with data gaps corrected with GTOPO30 data. SRTM30 pixels are 30" (approximately 1 km<sup>2</sup>). Data were processed by NASA's Jet Propulsion Laboratory and provided by the Earth Resources Observation Systems Data Center.

Stratigraphic and topographic considerations indicate that the northern segment of the Andes has been affected by both surface uplift and exhumation. Both tectonic and erosional processes drive uplift and exhumation of the nearby Cordillera Blanca. Tectonic exhumation is accomplished by the Cordillera Blanca normal fault, a 210-km-long active normal fault that defines the western edge of the range (McNulty and Farber 2002). Erosion is obvious in the high sediment flux in the rivers and significant number of active warm-based glaciers (Rodbell and Seltzer 2000). Long-term exhumation

of the Cordillera Blanca through both erosional and tectonic processes has occurred since 5–6 Ma (Perry and Garver 2004).

Low-temperature thermochronology in orogenic belts relies on dating techniques that record the temporal pace of rock cooling that can then be related to either exhumation processes or thermal events. One challenge is to find suitable thermochronometric dating methods that can address the temperature-time interval in question. In the Cordillera Huayhuash, the rocks are dominated by Mesozoic quartzites and carbonates with minor late

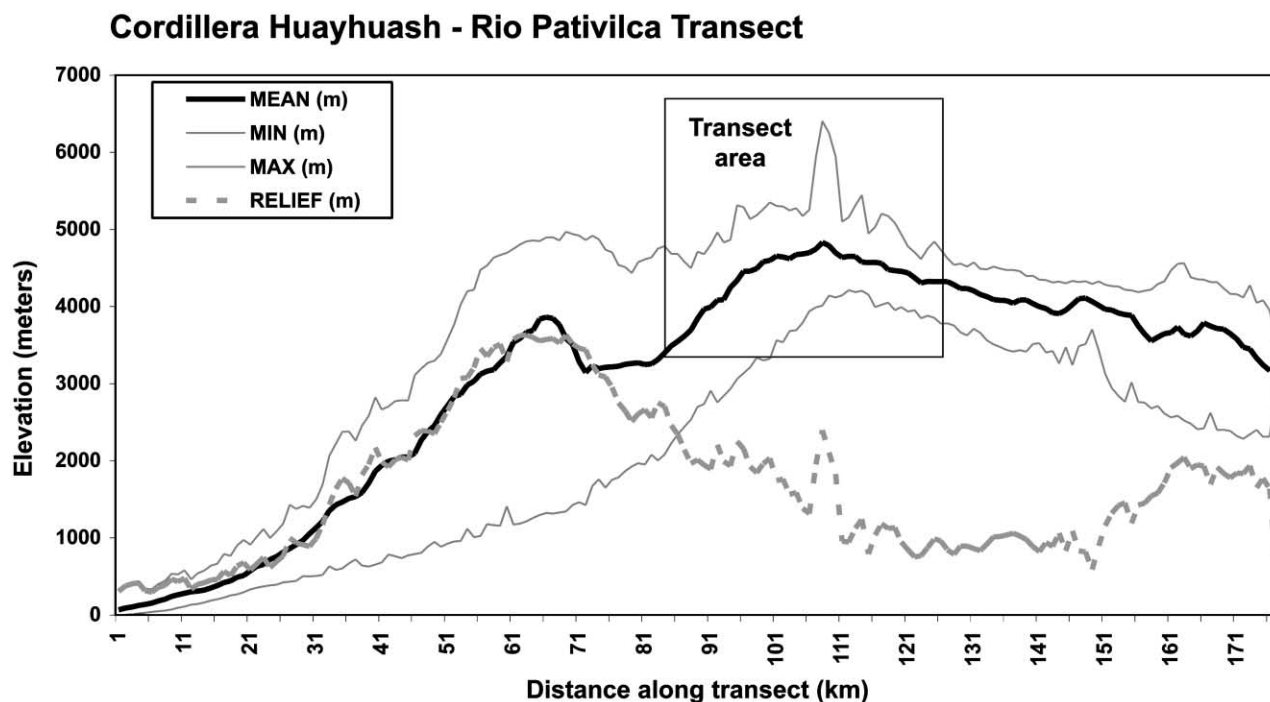


**Figure 3.** Aspects of topography taken from the 1-km digital elevation model of this area as indicated in figure 2. Shown are the minimum, mean, and maximum topography as well as the relief. Note that the study area is along the crest of this part of the Andes and occurs at the highest elevations. However, the western flanks of the range have greater total relief, which occurs in the form of very deeply incised canyons. Elevation data were extracted from a 50-km-wide swath along the transect shown in figure 2.

dikes. In this setting, the carbonate rocks are barren, but there are abundant detrital zircons in the quartzites. These zircons were deposited in the Cretaceous from a source with Late Paleozoic cooling ages, so most have considerable radiation damage (Schiffman 2003). Fission track (FT) analysis of radiation-damaged grains is routine, but there are some important issues with understanding the effect of radiation damage on thermal annealing and effective closure temperature of zircons (Garver et al. 2000). Helium dating of zircons is currently in a renaissance, and application to tectonic studies is still in its infancy (Reiners et al. 2002, 2003, 2004). As such, the relation of FT ages to He ages is important in establishing practical applications. One of the important aspects of this article is to review how radiation damage affects closure temperature of zircons and how low-temperature thermal events might result in complicated patterns of resetting.

### Geologic Background

Although the Andes appear to be a long, continuous mountain range with high average elevations, their

uplift history is complicated (Gregory-Wodzicki 2000). To determine the timing of crustal thickening and uplift of the Andes, several geologic lines of evidence have been studied, including paleobotanical proxies for temperature/elevation, geomorphic evidence bearing on the timing of canyon incision, and thermochronology of uplifted and exhumed rocks (Gregory-Wodzicki 2000). The thermochronologic studies have shown that the total extent of exhumation in the central Andes has been limited. Locally, however, FT cooling ages have implied two cooling events in the Eastern Cordillera and central Andes: one at 22 Ma and the second at 10–15 Ma (Benjamin et al. 1987; Laubacher and Naeser 1994). Note that although the interpretations of Benjamin et al. (1987) have been dissected by a number of workers in the literature, the basic conclusion remains valid: cooling rates increased significantly between 30 and 10 Ma in Bolivia (see Anders et al. 2002).

The northern Peruvian Andes sit above a non-magmatic part of the continental arc, which is inferred to reflect a low dip of the downgoing subducted oceanic lithosphere. This flat-slab sub-

duction is inferred to have initiated at ca. 5 or 6 Ma (McNulty and Farber 2002), but the evidence for this is weak and partly circular. It is likely that much of the final surface uplift of the Andes in northern Peru was attained in the last 5–6 m.yr. Regional mapping has refined our understanding of the geomorphic response to uplift since the Middle Miocene. Three erosional surfaces are recognized: the Puna, Vallé, and Cañon (Myers 1980; Cobbing et al. 1981, 1997). (1) The oldest is the Puna surface, which is widely recognized in the Andes (Bowman 1906; Tosdal et al. 1984; Coltorti and Ollier 1999), and is characterized by a nearly flat surface, now at 4200–4400 m. Geomorphic evidence suggests that uplift occurred in two stages because it is dissected by two erosional events (Wilson et al. 1967). Here, the Puna surface has developed on volcanics of the Eocene to Miocene Calipuy Group, which is as young as 15 Ma, and like elsewhere in Peru, it is assumed to have been cut at or near sea level. (2) The Vallé stage represents the first stage of valley incision, and these erosional surfaces cut the Puna surface. The Vallé stage was cut in response to the initial surface uplift of the Andes in northern Peru. A late-stage valley fill of the Forteleza (Formation) Ignimbrite is approximately 2000 m thick in the Forteleza drainage, suggesting at least this much relief had formed by 5–7 Ma. The Vallé stage of canyon cutting therefore occurred in the Middle to Late Miocene. (3) The Cañon stage represents the last stage of deep canyon incision into the Puna surface and the Vallé stage surfaces, and it accounts for approximately 2000–3000 m of incision. Because the Cañon incision cuts both the Vallé and Puna surfaces (and the ignimbritic units that fill the Vallé canyons), it is Pliocene to Recent.

The Cordillera Blanca, directly to the north of the Cordillera Huayhuash, consists mainly of an upper Miocene granodioritic batholith (McNulty et al. 1998). Soon after intrusion, the Cordillera Blanca Batholith was uplifted along with the rest of the Andes. Along the west margin of the mountain range, the west-dipping Cordillera Blanca normal fault extends for ~210 km along the range. Since 6 Ma, rapid rock uplift and exhumation of the Cordillera Blanca occurred (Garver et al. 2003; Schiffman 2003; Perry 2004; Perry and Garver 2004). One interpretation is that exhumation of the Cordillera Blanca was driven by uplift of the Andes and that deep-level exhumation occurred along the axis of Miocene plutonism. This exhumation coincides with the inferred initiation of flat-slab subduction in this segment of the Nazca subduction zone (fig. 1; McNulty and Farber 2002).

The Cordillera Huayhuash can be viewed as the

southern continuation of the Cordillera Blanca in terms of both its topographic and intrusive setting, and rocks of the Cordillera Blanca have a similar pre-Neogene structural history that bears on our cooling ages (Megard 1987; Sébrier et al. 1988). A belt of Miocene plutons can be traced from the Cordillera Blanca, south along the drainage divide into the Cordillera Huayhuash. The bedrock in the Cordillera Huayhuash can be grouped into four main geologic units (summarized from Coney 1971): (1) Mesozoic rocks, mainly Cretaceous carbonates and quartzites, folded and thrust-faulted between the Turonian and the Middle(?) Tertiary. By the Middle Tertiary, 50% of the folded rock was eroded, and an unconformity developed with overlying thin, poorly dated red beds. At the same time, intrusion of the Late Cretaceous Coastal Batholith occurred to the west (Cobbing et al. 1997). (2) The Tertiary Calipuy Formation comprises volcanic rocks erupted regionally between 30 and 15 Ma and has an estimated thickness of 2000–3000 m (Coney 1971; Wilson et al. 1995; Cobbing et al. 1997). These Tertiary rocks rest unconformably on the underlying folded and eroded Cretaceous thrust belt and locally heated rocks of the thrust belt (Perry 2004). (3) In the Miocene, the entire sequence was intruded by granitic plutons. (4) Finally, as recently as 6 Ma (during the Mio-Pliocene), explosive silicic volcanism occurred. In the Cordillera Huayhuash, this event resulted in the deposition of the Puscanturpa Volcanics and related feeder dikes. Elsewhere, these may be correlated to the Yungay volcanic rocks to the north and west and the Forteleza Formation to the west and the Huayllay Formation to the east (Coney 1971; Wilson et al. 1995; Cobbing et al. 1997). Because the Puscanturpa Formation (Huayllay Formation) erupted on a nearly flat, beveled surface (Coney 1971), it plays an important role in understanding the young exhumation history of the area.

**Low-Temperature Thermochronology.** Fission-track dating of apatite and zircon is commonly used to address the timing of rock cooling in orogenic systems. More recently, (U-Th)/He dating on apatite and zircon has been used in conjunction with FT dating to obtain more detailed thermal histories accompanying exhumation.

Fission tracks in zircon are formed from the spontaneous fission of  $^{238}\text{U}$ . At elevated temperatures, these tracks anneal and disappear as fast as they are formed, but at low temperatures, tracks are fully retained. The temperature below which tracks are retained and above which tracks are lost is commonly referred to as the partial annealing zone (PAZ). The effective closure temperature is depen-

dent on the cooling rate but is usually close to the temperature of nearly full track retention and therefore closure of the FT system. In typical geological settings, zircon has an effective closure temperature of about  $250^\circ \pm 40^\circ\text{C}$  (Brandon et al. 1998), but this estimate is sensitive to the rate of cooling and radiation damage in the zircon. High radiation damage lowers the annealing temperature, and in some cases, tracks may be annealed and the grain reset at temperatures of ca.  $200^\circ\text{C}$  or below (Garver et al. 2002; Rahn et al. 2004).

Accumulation and retention of helium in zircon are a function of the  $\alpha$  decay of uranium and thorium, He ejection, and He diffusion properties of that mineral. Zircon is a relative newcomer to routine practical use, but it is known to have an effective closure temperature of  $180^\circ \pm 20^\circ\text{C}$  (Reiners et al. 2002, 2003, 2004) for typical crystal sizes and cooling rates of about  $10^\circ\text{C}/\text{m.yr.}$  As with fission tracks, the retention of helium is dominated by thermal effects. The helium partial retention zone (PRZ) is analogous to the fission track PAZ; both represent the temperature conditions at the limit of daughter preservation. The former is the retention of helium in the host crystal, and the latter is the annealing or shortening of fission damage in the host crystal. During the production of helium, a He nucleus is ejected from the parent isotope and transported 15–20  $\mu\text{m}$  from the site of decay. This  $\alpha$  ejection is the source of a unique aspect of helium dating because when  $\alpha$  decay occurs near the edge of a host crystal, the  $\alpha$  particle can be ejected from it, and therefore some of the daughter isotope is lost from the system. As such, helium dating requires an  $\alpha$ -ejection correction, which can typically be treated as a function of the surface-area-to-volume ratio of the crystal (Farley et al. 1996; Farley 2002).

**FT Annealing of Radiation-Damaged Zircon.** Here we review aspects of radiation damage in zircon because this damage affects thermal annealing of the FT system. Individual zircon grains of mixed provenance have different total accumulated radiation damage depending on U + Th concentration and the length of time since first cooling and subsequent thermal history. Radiation damage in a zircon crystal consists of fission damage from U and  $\alpha$  recoil damage from both U and Th. Although fission damage produces relatively large zones of disorder associated with two heavy fission fragments, the low fission decay rate results in less accumulated damage compared with  $\alpha$  damage.

Radiation damage results in accumulated disorder in the crystal, and as damage increases with time, a zircon crystal is eventually transformed

from fully crystalline to amorphous (metamict). The crystalline-to-metamict transition is regarded as the point at which the zircon becomes x-ray amorphous and occurs at ca.  $5 \times 10^{15}$   $\alpha$  events/mg (Ellsworth et al. 1994; Ewing 1995). Once metamict, a crystal is so damaged that its material properties resemble a glass—complete disorder (Nasdala et al. 2004). In a practical sense, zircon at or near the crystalline-to-metamict transition has too

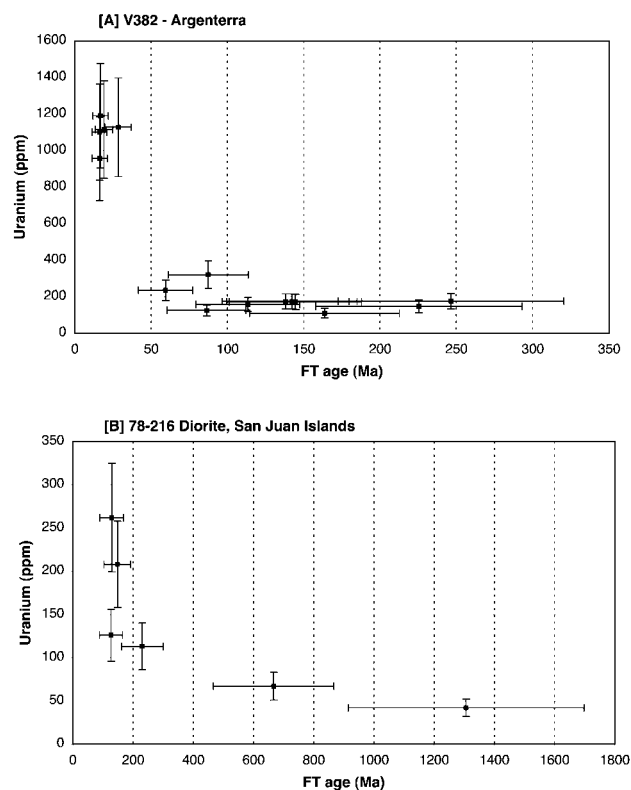


**Figure 4.** Plots showing uranium and single-grain fission track age for two single-source samples with wildly disparate grain ages. These grain-age distributions are attributed to heterogeneous radiation damage and variable retentivity. In both cases, grain age and uranium covary as is normally expected because age is derived from the uranium concentration, but the variation in these two samples is well beyond what is normally seen in single-source grain age distributions. In both cases, the young age of grains is inferred to represent the time of latest heating, and the older ages trail back to an original cooling age. Note that for a full calculation of radiation damage, one needs to know thorium concentration, but to a first order, uranium is a good proxy because in most typical cases, it accounts for 80%–90% of the radiation damage (Garver and Kamp 2002). *A*, Passo Ratticosa (Italian Alps) data from J. A. Vance, unpublished data. *B*, Data from Nanaimo Group from C. Naeser (pers. comm., 2003). Errors shown are 1 $\sigma$  estimates.

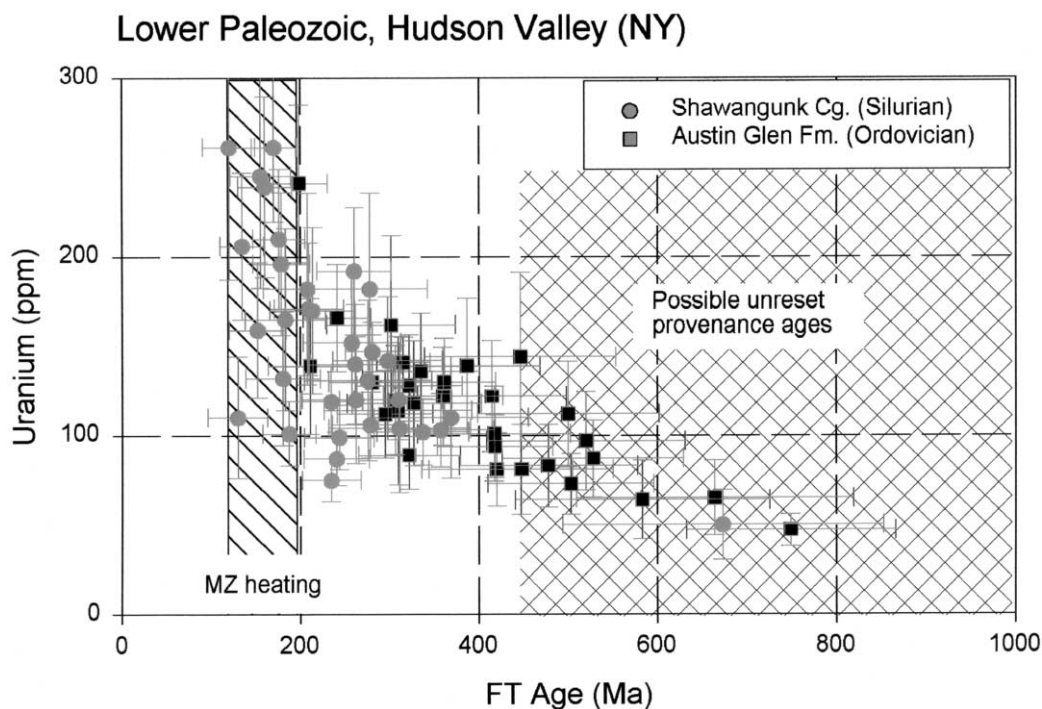


**Figure 5.** Fission track (FT) age distribution of reset single detrital zircon grains from the Shawangunk Conglomerate and the Austin Glen Formation in the Hudson Valley of New York state. These FT ages are largely younger than depositional age, and therefore most of the provenance information is lost. Two populations suggest thermal resetting in the Late Paleozoic and in the Early Jurassic. Published vitrinite reflectance (VR), conodont alteration index, and illite crystallinity values suggest that rocks in this part of the Hudson Valley experienced temperatures of ca. 180°–220°C. VR values are reported between 2.0% and 2.5% ( $R_0$ ; Garver and Bartholomew 2001). Errors shown are  $1\sigma$  (from Garver et al. 2000; Garver and Bartholomew 2001).

much damage to have FTs etched and revealed under ordinary laboratory conditions (Garver and Kamp 2002). However, transitional zircon (between crystalline and amorphous) has enough damage to have altered the physical properties of the material.

In a study of radiation-damaged grains in the Southern Alps of New Zealand, Garver and Kamp (2002) defined ranges of practical radiation damage in typical detrital zircon suites. This scheme includes crystalline, transitional, and metamict fields in the temporal evolution of typical ranges of U + Th (or “eU”) in zircon (Garver and Kamp 2002). The change from crystalline to transitional state occurs after about 2–5 m.yr. for zircons with typical eU (200–750 ppm; Garver and Kamp 2002). For zircon fission track (ZFT) cooling ages of  $\leq 5$  Ma, accumulated radiation damage for a typical grain would be ca.  $5 \times 10^{12}$   $\alpha$  events/mg, whereas the onset of metamictization is inferred to occur at ca.  $5 \times 10^{15}$   $\alpha$  events/mg (Chakoumakos et al. 1987), which would require several billion years for a typical zircon.

Note that the term “detrital suites of zircons” implies an assemblage of zircon deposited with a range of original cooling ages and a wide range of eU, and therefore there is a wide range of radiation damage from grain to grain (Garver et al. 2000). If a suite contains syndepositional, volcanic-derived grains (i.e.,  $<50$  k.yr. at deposition) and Proterozoic grains of typical composition, the likely range of radiation damage from grain to grain might span six orders of magnitude from  $10^9$  to  $10^{15}$   $\alpha$  events/mg, presumably common in detritus from most modern active continental arcs.

Field studies reveal that some zircons have high retention and some have low retention of fission tracks, and it is likely that this difference is caused by differences in accumulated radiation damage (figs. 4, 5). High retentive zircons (HRZs) close at relatively high temperatures, and they are inferred to be relatively resistant to annealing after cooling. Low retentive zircons (LRZs) have a low effective closure temperature and a low resistance to annealing. Several studies have shown that ZFT

grains from a single zircon sample may span hundreds of millions of years because end member grains record different thermochronologic events (fig. 4; see also Seward and Rhodes 1986; Carter 1990; Laubacher and Naeser 1994; Garver et al. 2002; C. W. Naeser, pers. comm., 2003).

The effects of radiation damage on He retention, and therefore resetting properties of ZHe ages, are not well understood. Two studies suggest that He diffusion from zircons may not be significantly affected until unusually high  $\alpha$  dosages. Nasdala et al. (2004) measured ZHe ages on a suite of detrital zircons with the same U/Pb ages (and inferred thermal histories) but strongly contrasting U concentrations (288–5670 ppm) and found that only zircons with  $\alpha$  doses greater than about  $2\text{--}3 \times 10^{18}$   $\alpha$ /mg showed anomalously young ages, presumably caused by high He diffusivity (Nasdala et al. 2004). Reiners et al. (2004) also showed that zircons with long-term low-temperature thermal histories and strongly contrasting accumulated  $\alpha$  doses ( $4 \times 10^{16}$  vs.  $1.5\text{--}2.0 \times 10^{18}$   $\alpha$ /mg) displayed no discernible differences in He diffusion properties.

To illustrate the dramatic effect  $\alpha$  damage can have on ZFT ages in natural samples, we show two examples of the resetting of high-radiation damaged (LRZ) grains (fig. 4). The first example (fig. 4) shows results from two different studies of plutonic rocks, where all grains experienced the same thermal history and the same starting point for  $\alpha$  damage. In these cases, grain ages from a single granite clast span more than 100 m.yr., and young ages are from high uranium grains. The implication here is that after an initial cooling event, zircons accumulate radiation damage at rates proportional to their U (and Th) concentrations. Once reheated, only more damaged grains were reset and recorded the young event. Another example comes from zircons from lower Paleozoic sandstones in the Hudson Valley (New York; fig. 5). These samples show three main age clusters: (a) reset Early Jurassic ages ( $\sim 185$  Ma), (b) reset or partially reset in the Late Paleozoic (ca. 275–322 Ma), and (c) unreset to partially reset in the Early Paleozoic (Garver and Bartholomew 2001). These young reset ages coincide with known thermal events in this area, and published thermal estimates suggest that rocks in this area experienced temperatures of ca. 180°–220°C (fig. 5). This and two similar settings have been used to estimate that low-temperature resetting may have a threshold value of ca.  $5 \times 10^{13}$   $\alpha$  events/mg (i.e., a typical grain cooled for 100 m.yr. with 225 ppm eU; Garver et al. 2000).

Annealing of radiation damage is temperature and time dependent, but the exact processes of

damage repair in a crystal are poorly understood. Two end members of naturally annealed radiation damage in detrital suites have been reported in the literature. The first is full annealing, in which rocks with detrital suites of zircons are brought to temperatures sufficient to fully anneal all zircons, regardless of inherited radiation damage. In this case, LRZs and HRZs are fully annealed and reset to a common cooling age. Studies of rapidly cooled rocks of the Southern Alps in New Zealand suggest that temperatures in excess of 300°C are required for this extent of annealing (Green et al. 1996; Tagami et al. 1998). The second is full annealing of LRZs, where only the less retentive grains are reset and the high-retentive grains are not reset or are only partly reset. In this latter case, it is unclear whether the HRZs are partially annealed or completely unannealed. Partial annealing would result in a reduction of track lengths and therefore a reduction in the apparent age of a crystal. Heated rocks (ca. 200°C) in a Laramide basin in Arizona have reset LRZs but have not reset HRZs because the HRZs had similar population distributions between heated and nonheated samples (Riley and Garver 2002; Riley 2003).

Etch times of fully reset samples are inferred to be a proxy for the presence or absence of  $\alpha$  damage (Brandon and Vance 1992). Long etch times imply a more crystalline structure and therefore little radiation damage. Because this relationship seems to hold for those rocks with fully reset samples (both LRZs and HRZs), it has long been assumed that  $\alpha$  damage and fission damage are thermally annealed at more or less the same temperature. While this general relationship may hold for fully reset samples, this is not the case for the resetting of LRZs. In this case, thermal resetting of LRZs occurs before annealing of the majority of  $\alpha$  damage in a grain (Riley and Garver 2002). Therefore, in samples heated to ca. 200°C, fission tracks in LRZs are reset, but  $\alpha$  damage is not. Several observations support this inference, but most important are actual measurements of crystalline disorder using single-grain Raman spectroscopic studies (Riley and Garver 2002). Young reset grains have appreciable  $\alpha$  damage, well over what would be expected if  $\alpha$  damage and fission damage were reset at the same time. The conclusion from this work is that fission tracks in LRZs can be annealed without significant resetting of  $\alpha$  damage (Riley 2003).

Described previously are two end member situations with respect to the thermal resetting of fission tracks and  $\alpha$  damage in zircons. One end member is where LRZs are reset at relatively low temperatures without appreciable resetting of  $\alpha$

**Table 1.** Summary of Zircon Fission Track Data from Cordillera Huayhuash

Sample	Elevation (m)		$\rho_s$ (cm <sup>2</sup> )	$N_s$	$\rho_i$ (cm <sup>2</sup> )	$N_i$	$\rho_d$ (cm <sup>2</sup> )	$N_d$	$n$	$\chi^2$ (%)	Age	$-1\sigma$	$+1\sigma$	$U \pm 2$ SE
Quartzites:														
		Unreset												
03-25	4026	Zircon	$8.10 \times 10^6$	1261	$2.26 \times 10^6$	352	$3.165 \times 10^5$	1880	35	.0	170.7	-11.8	+12.7	$87.9 \pm 10.1$
03-28	4000	Zircon	$6.86 \times 10^6$	747	$1.64 \times 10^6$	178	$3.053 \times 10^5$	1797	20	1.4	233.1	-19.2	+20.9	$65.9 \pm 10.2$
		Partially reset												
03-13	2900	Zircon	$5.57 \times 10^6$	932	$3.25 \times 10^6$	544	$3.024 \times 10^5$	1780	30	.0	67.6	-4.8	+5.2	$132.2 \pm 12.8$
03-14	2760	Zircon	$3.10 \times 10^6$	423	$3.51 \times 10^6$	479	$2.993 \times 10^5$	1761	30	.0	44.5	-3.2	+3.5	$144.3 \pm 14.6$
03-15	3240	Zircon	$8.08 \times 10^6$	835	$2.42 \times 10^6$	250	$2.962 \times 10^5$	1743	20	.1	169.2	-12.8	+13.8	$100.4 \pm 13.4$
03-16	4070	Zircon	$7.23 \times 10^6$	1166	$3.80 \times 10^6$	613	$2.931 \times 10^5$	1670	35	.0	40.3	-3.9	+4.4	$159.6 \pm 14.4$
03-24	4036	Zircon	$7.49 \times 10^6$	898	$3.55 \times 10^6$	426	$3.222 \times 10^5$	1896	20	.0	99.1	-6.9	+7.4	$135.7 \pm 14.5$
		Reset												
03-19	4235	Zircon	$1.03 \times 10^6$	178	$5.03 \times 10^6$	867	$2.854 \times 10^5$	1679	15	49.5	10.9	-.9	+1.0	$216.9 \pm 16.9$
03-22	4400	Zircon	$9.40 \times 10^5$	184	$4.08 \times 10^6$	798	$2.968 \times 10^5$	1748	20	84.7	12.7	-1.0	+1.1	$169.0 \pm 13.5$
03-23	4653	Zircon	$9.20 \times 10^5$	96	$3.20 \times 10^6$	334	$2.912 \times 10^5$	1715	15	97.4	15.6	-1.7	+1.9	$135.2 \pm 15.6$
Granites:														
03-17	4210	Zircon	$9.97 \times 10^5$	180	$4.92 \times 10^6$	888	$2.900 \times 10^5$	1707	15	18.4	10.9	-.9	+1.0	$208.6 \pm 16.2$
03-18	4235	Zircon	$1.02 \times 10^6$	199	$4.92 \times 10^6$	959	$2.869 \times 10^5$	1688	15	91.4	11.1	-.9	+.9	$210.9 \pm 15.8$
Volcanics:														
03-26	4355	Zircon	$5.43 \times 10^6$	363	$4.28 \times 10^6$	286	$3.081 \times 10^5$	1814	8	.0	22.2	-3.8	+4.4	$170.7 \pm 21.3$
03-27	4145	Zircon	$9.98 \times 10^5$	152	$8.56 \times 10^6$	1304	$2.855 \times 10^5$	1682	15	55.1	6.2	-.5	+.6	$368.9 \pm 24.2$

Note.  $\rho_s$  = density of spontaneous tracks;  $N_s$  = number of spontaneous tracks counted;  $\rho_i$  = density of induced tracks;  $\rho_d$  = density of tracks on the fluence monitor (CN5);  $n$  = number of grains counted. Fission track ages ( $\pm 1\sigma$ ) were determined using the  $\zeta$  method, and ages were calculated using the computer program and equations in Brandon (1996). All ages with  $\chi^2 > 5\%$  are reported as pooled ages; otherwise,  $\chi^2$  are shown. For zircons, a  $\zeta$  factor of  $348.45 \pm 6.51$  ( $\pm 1$  SE; L. J. Walker) is based on determinations from both the Fish Canyon Tuff and the Buluk Tuff zircons. Glass monitors (CN5 for zircons), placed at the top and bottom of the irradiation package, were used to determine the fluence gradient. All samples were counted at  $1250\times$  using a dry  $100\times$  objective ( $10\times$  oculars and  $1.25\times$  tube factor) on an Olympus BMAX 60 microscope fitted with an automated stage and a digitizing tablet.

**Table 2.** Summary of Component Populations, Huayhuash Transect

Sample	Unit	Age	$n$	P1	P2	P3	P4
03-13	Oyon Formation	Lower Cretaceous (Valanginian)	30	33.2 -8.3/+11.0 8.9%	64.7 -8.7/+10.0 31.7%	134.9 -14.7/+16.5 59.3%	...
03-14	Chicama Formation	Upper Jurassic	30	24.4 -4.1/+4.9 29.7%	56.8 -5.6/+6.3 66.9	... ... ...	250.9 -114/+206 3.4
03-15	Chimu Formation	Lower Cretaceous (Valanginian)	20	... ... ...	... ... ...	113.8 -16.2/+18.9 50.9%	242.2 -31.1/+35.6 49.1%
03-28	Chimu Formation	Lower Cretaceous (Valanginian)	20	... ... ...	... ... ...	159.3 -39.5/+52.3 48.2%	299.0 -64.9/+82.3 51.8%
03-25	Oyon Formation	Lower Cretaceous (Valanginian)	35	... ... ...	47.0 -10.7/+13.8 6.3%	192.1 -21.5/+24.1 73.6%	322.7 -71.8/+91.7 20.1%
03-24	Carhuaz Formation	Lower Cretaceous (Hauterivian-Barremian)	20	... ... ...	66.1 -7.7/+8.7 22.7%	116.5 -28.4/+37.4 37.1%	216.7 -38.0/+45.9 40.1%
03-16	Chimu Formation	Lower Cretaceous (Valanginian)	35	26.9 -3.8/+4.4 9.1%	68.3 -8.1/+9.2 24.9%	148.6 -23.3/+27.6 66.0%	...
03-19	Carhuaz Formation	Lower Cretaceous (Hauterivian-Barremian)	15	10.9 -0.9/+1.0 100%	... ... ...	... ... ...	...
03-22	Carhuaz Formation	Lower Cretaceous (Hauterivian-Barremian)	20	12.7 -1.0/+1.1 100%	... ... ...	... ... ...	...
03-23	Carhuaz Formation	Lower Cretaceous (Hauterivian-Barremian)	15	15.6 -1.7/+1.9 100%	... ... ...	... ... ...	...
03-18	Unnamed granite	Miocene(?)	15	11.1 -0.9/+0.9 100%	... ... ...	... ... ...	...
03-17	Unnamed granite	Miocene(?)	15	10.9 -0.9/+1.0 100%	... ... ...	... ... ...	...

Note.  $n$  = number of grains counted. Binomial peak-fitted components determined from routine outlines in Brandon (1996). For all samples that pass  $\chi^2$ , the  $\chi^2$  age is given as P1. Table excludes volcanics because they are unrelated to cooling associated with heating/exhumation.

damage, and another is where all FTs and  $\alpha$  damage are reset fully in LRZs and HRZs at higher temperatures. Note that these observations are important because the amount of  $\alpha$  damage affects track revelation and the thermal stability of FTs. At this point, we need to consider the complicated issue of the temperature bounds of these end member situations.

**Temperature Bounds of Annealing.** The zircon partial annealing zone (zPAZ) is well described in the literature (Brandon et al. 1998 and references therein). Traditionally, the zPAZ is viewed as the temperature bounds that define track stability and retention of tracks in nature. While the general temperature limits of the zPAZ are known, there is disagreement in the details and applicability to natural settings. This disagreement can be attributed to a difference between the annealing char-

acteristics of either radiation-damaged zircon (i.e., LRZs) and more crystalline zircon (i.e., HRZs). The controversy exists because the temperature at the base of a modern zPAZ has not been measured directly; it is inferred to lie above 255°C (i.e., Coyle and Wagner 1996; Bernet 2002; Brix et al. 2002; Thomson 2002). A kinetic model based on laboratory-scale zircon annealing experiments, fit to several zircon FT data sets from boreholes, predicts a temperature of about 310°C for the base of a zPAZ (Tagami et al. 1998). The temperature at the top of the zPAZ is inferred to be >200°–210°C based on the zircon FT ages and lengths at the base of deep boreholes (Green et al. 1996; Tagami et al. 1996). The fitted kinetic model of Tagami et al. (1998) suggests a temperature close to 210°C for the top (low temperature) of the zPAZ for 10-m.yr. heat-

**Table 3.** (U-Th)/He Dating of Single Zircon Grains from the Cordillera Huayhuash

Sample	Elevation (m a.s.l.)	Map unit	Latitude	Longitude	Mass ( $\mu\text{g}$ )	SGHW ( $\mu\text{m}$ )	$^4\text{He}$ (ncc STP)	U (ppm)	Th (ppm)	Th/U	Raw age (Ma)	HAC	Age (Ma)	$2\sigma$ err (Ma)
03-16A	4070	Ki-Ch	10°14.351	76°57.099	11.9	47.8	5.385	171	135	.79	18.4	.795	23.2	1.85
03-16B	4070	Ki-Ch	10°14.351	76°57.099	3.39	34.8	.669	223	67.6	.30	6.83	.716	9.54	.76
03-19A	4235	Ki-C	10°13.813	76°55.871	7.70	44.8	.797	123	110	.90	5.74	.774	7.42	.59
03-19B	4235	Ki-C	10°13.813	76°55.871	8.95	47.5	.626	63.9	41.9	.66	7.85	.786	9.99	.80
03-22A	4400	Ki-C	10°15.203	76°56.393	2.19	26.8	.116	86.2	38.3	.44	4.62	.657	7.03	.56
03-24A	4036	Ki-C	10°13.965	76°59.544	6.32	37.0	1.226	166	92.8	.56	8.52	.746	11.4	.91
03-24B	4036	Ki-C	10°13.965	76°59.544	7.39	45.8	1.121	135	31.7	.24	8.83	.778	11.4	.91

Note. (U-Th)/He dating was done on single zircon grains heated by a Nd:YAG laser, and then the dissolved zircon was analyzed using a Finnigan Element2 inductively coupled plasma-mass spectrometer (ICP-MS). HAC =  $\alpha$  ejection correction (Ft of Farley 2002). SGHW = single-grain half-width of the tetragonal prism face. Each zircon was photographed, measured, and wrapped in Pt foil. Samples were degassed with a Nd:YAG laser for 15 min at ca. 1100°–1300°C; quantitative He release was checked by reextractions. Gas was spiked with  $^3\text{He}$ , concentrated and purified in a cryotrap cycling between 16 and 37 K, and measured on a quadrupole mass spectrometer. Degassed zircons then were plucked from the Pt foil, placed in Teflon microvials with  $^{229}\text{Th}$  and  $^{233}\text{U}$  spike, HF, and  $\text{HNO}_3$ , and digested at 225°C for 3 d. The vials were then removed from the bomb, and the HF and  $\text{HNO}_3$  were evaporated, and HCl was added and then heated for 24 h at 200°C. The single-grain solutions were analyzed on a Finnigan Element2 ICP-MS (Reiners et al. 2004). Ki-Ch is the lower Cretaceous Chimú Formation, and Ki-C is the lower Cretaceous Carhuaz Formation.

ing. Note, however, that these experiments had a narrow window for etch time, so it is possible that reset, hard-to-etch grains were missed. As such, these thermal estimates are likely an overestimation of the low-temperature bound for LRZs. We would like to underscore this point: etch procedure affects the result in studies with any grain-to-grain variation in radiation damage. If a procedure is optimized to reveal tracks in relatively old track-rich grains, young reset grains may be entirely missed because they might have required a significantly longer etch time.

A number of studies suggest that the thermal stability of FTs decreases with increasing  $\alpha$  damage, and these studies give a slightly different result for the bounds of the zPAZ (Kasuya and Naeser 1988; Rahn et al. 2004). Studies on reset, radiation-damaged zircons in heated strata of the Olympic Peninsula (Washington) indicate that the upper and lower bounds for the zPAZ are closer to 180°–240°C for 10-m.yr. heating (Brandon et al. 1998). These estimates represent 10% and 90% annealing isopleths (approximately the top and bottom of a PAZ) for reset zircon grains with that greatest susceptibility to thermal annealing. These observations indicate that the zPAZ is clearly an oversimplification for most settings with natural radiation-damaged zircon. The annealing bounds of any single zircon depend on the time-temperature history of the host rock and the degree of radiation damage of a zircon. As such, there is probably an infinite number of partial annealing zones for a suite of heated detrital grains that have accumulated radiation damage.

With this background, we turn to the thermal resetting of zircons from quartzites from the Cordillera Huayhuash in northern Peru. Here, we

know depositional age (ca. 100 Ma), and we know that correlative rocks that have remained at high levels in the crust retain zircon FT cooling ages as old as 300 Ma. Hence, by the Late Tertiary, these zircons had accumulated significant but variable levels of radiation damage.

### Methods and Results

Zircon crystals were extracted from 2–4-kg rock samples and analyzed using standard procedures for the external detector method (Naeser 1979), and FT ages were calculated for each sample using the  $\xi$  method (table 1). For samples with multiple populations of grain ages, populations were evaluated using a binomial peak-fitting routine (table 2). For ZHe dating, duplicate single-grain crystals from each sample were processed. Two zircons from four samples were selected based on size and euhedral shape. Each zircon was measured and wrapped in platinum foil that was then lightly crimped. Samples were degassed with an Nd:YAG laser for 15 min at ca. 1100°–1300°C. The released gas was then spiked with  $^3\text{He}$  and trapped in the Cryotrap and analyzed in a quadrupole mass spectrometer. Zircons were then removed from the Pt foil, spiked with a calibrated  $^{229}\text{Th}$  and  $^{233}\text{U}$  solution, dissolved in Parr bomb at 225°C, and analyzed using sector inductively coupled plasma-mass spectrometer (ICP-MS) for U-Th (table 3).

The FT ages from quartzites have a wide range of ages from 10 to more than 200 Ma. Almost all of them fail  $\chi^2$ , indicating that there is a range of grain ages greater than expected for a single coherent population of FT ages. Binomial peak fitting provides single peak ages from 11 to 322 Ma, with populations falling into several groups (table 2). The

## Simplified Geology of the western Huayhuash Range, northern Perú

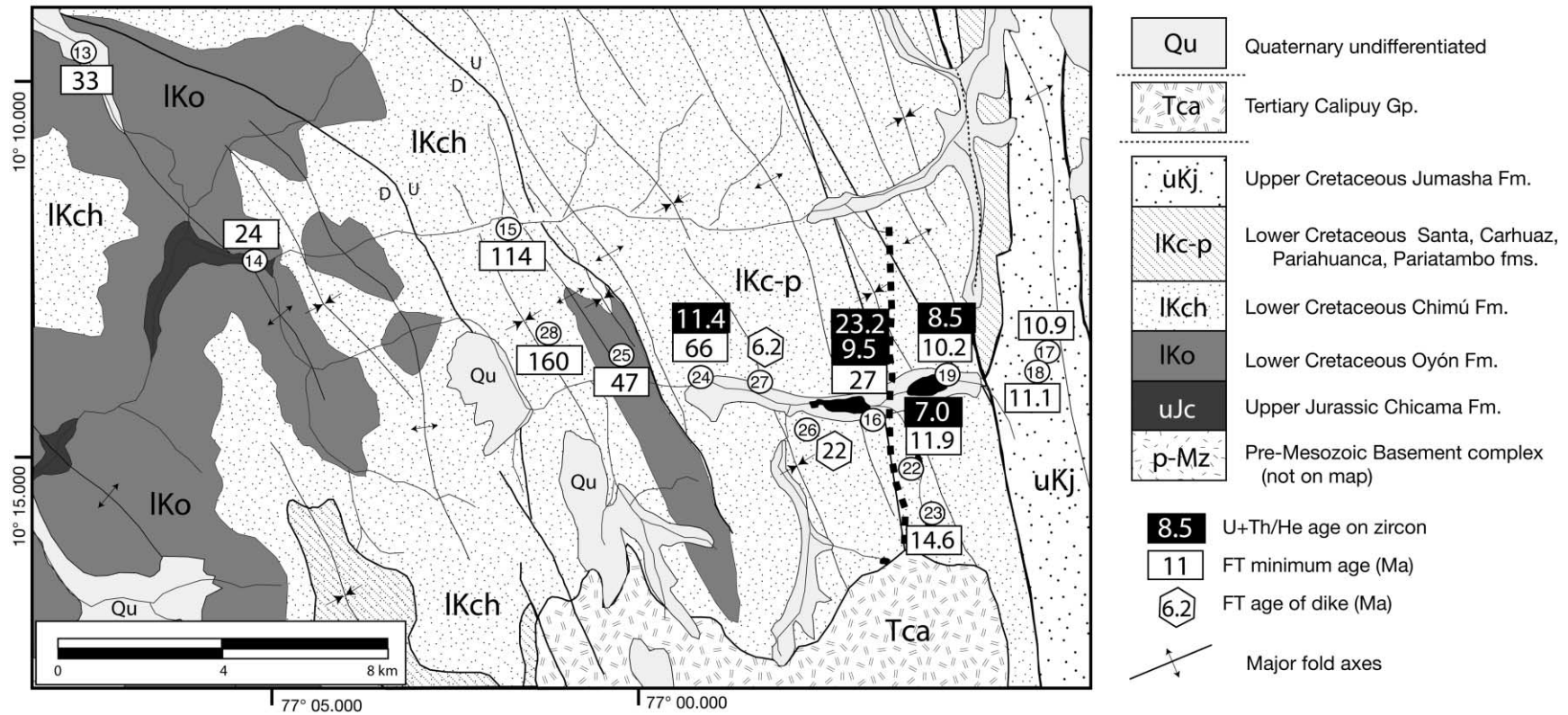


**Figure 6.** Simplified geologic map of the northwest part of the Huayhuash Range, northern Peru. Map base from Cobbing et al. (1997). Dashed line separates samples with zircon fission track (ZFT) ages that are partially annealed (to the west) and fully annealed (to the east). ZFT minimum ages and ZHe ages are given in tables 2 and 3, respectively. The Tertiary Calipuy Group (*Tca*) is regionally mapped as the Calipuy Group but is referred to as the Tscara Volcanics. Circled numbers are sample locations.

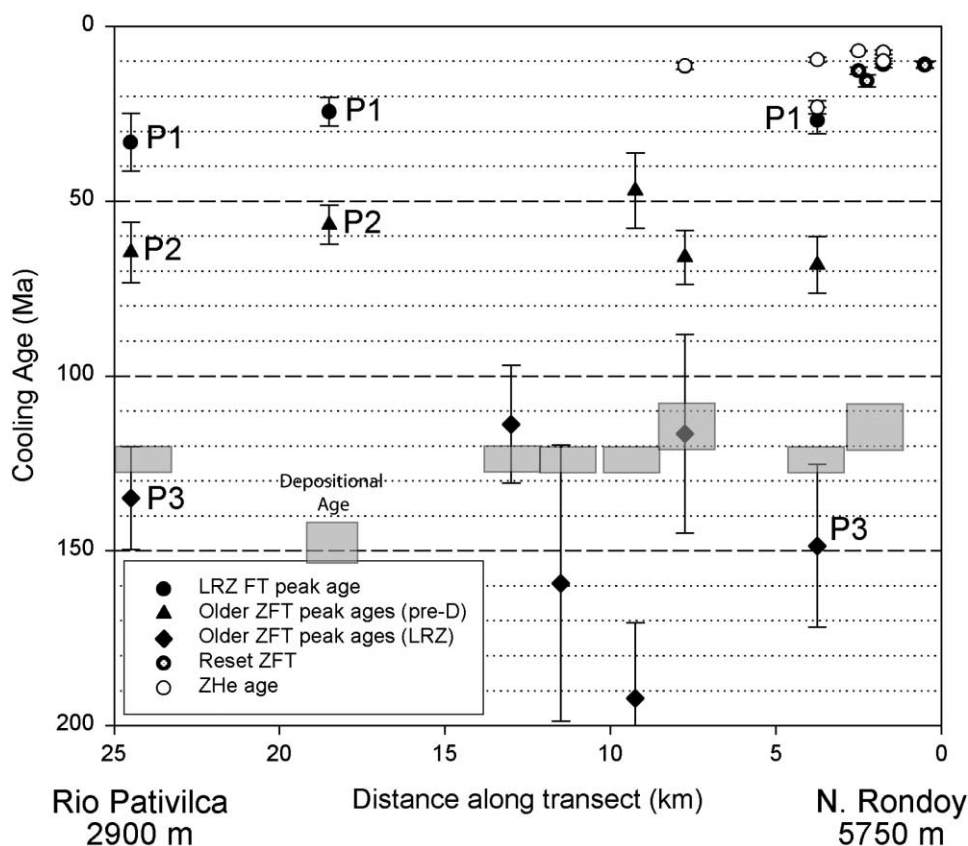


**Figure 7.** Plot showing zircon fission track and ZHe ages (*open circles*) along transect from the Rio Pativilca to the core of the Huayhuash.

FT ages of granitic rocks from the central part of the range are 11.1–10.9 Ma. The FT ages of the hornblende-phyric volcanics are 22.2 Ma, but this age is poorly defined because it is based on marginal grains. The FT age of the quartz-rich felsic dike is 6.2 Ma, and it is based on excellent zircons. He ages range from 7 to 23 Ma, with most falling between 9 and 11 Ma (table 3).

Two coal samples from the central part of the transect (near samples 03-24 and 03-25) were analyzed for vitrinite reflectance ( $R_o$ ) and organic maturation. The samples are from seams with pervasive slip surfaces, so they had clearly been tectonically reworked. Maximum  $R_o$  values for 03-24 are 1.68, and sample 03-25 has a bimodal distribution of values, one at  $R_o = 1.81$  and the other at  $R_o = 4.7$ .

### Discussion

**FT Ages.** The resetting pattern varies with distance from the central high topography of the Huayhuash. Two and one-half kilometers from the

central uplift, samples are fully reset with peak ages between 10 and 15 Ma (reset ages; figs. 6, 7, 8). Between 24.5 and 2.5 km, samples have multiple peak ages, and many have peak ages younger than deposition (partly reset ages). Only two samples have peak ages that are older than or equal to deposition (unreset ages), which would suggest that they retain provenance information.

**Unreset Ages.** These ages can be used to understand the provenance of the rocks because they retain information about the cooling history of the source. Because the samples are mature quartz arenites, presumably from a mature source, we would expect cooling ages to be much older than deposition, and these cooling ages represent the thermal evolution of the source (see nos. 15 and 28 in fig. 6). The older peak, between 242 and 299 Ma, comprises half the grain ages, which is not uncommon in these suites. Schiffman (2003) reported a detrital age of 279 Ma from a similar unreset unit in the Cordillera Blanca.

**Reset LRZ.** These samples have a young peak age that represents the most recent cooling episode.

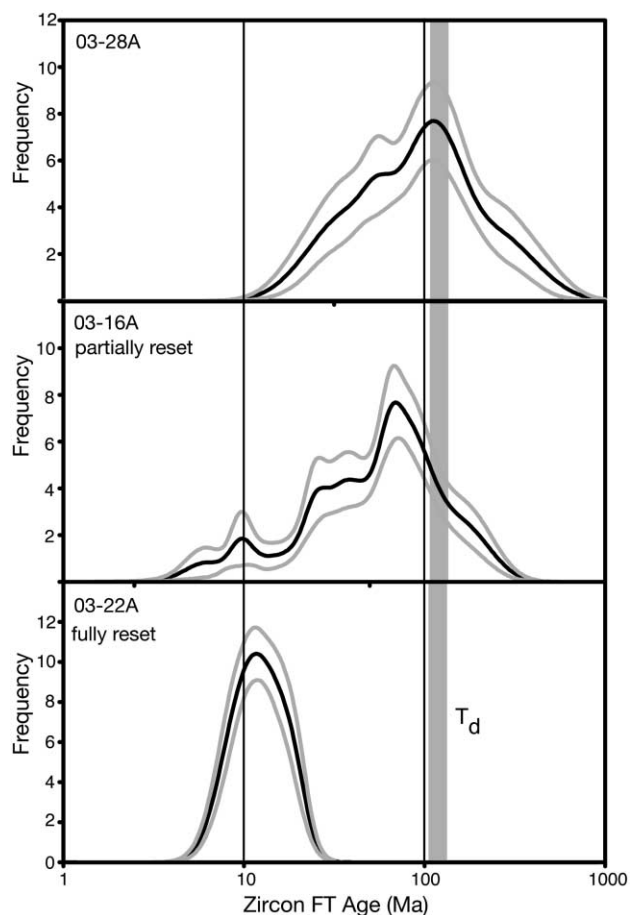


**Figure 8.** Probability density plots of mostly unreset, partly reset, and fully reset zircons from Cretaceous quartzites in the Cordillera Huayhuash. In the middle diagram, which shows a sample that has a wide range of grain ages, many younger than depositional age, note that some grains are reset and others are not. This sample retains old grains that are presumably high retentive zircon (HRZ), some grains that are partly reset (mid-Tertiary), and a small component of low retentive zircon (LRZ) that are full reset at ca. 10 Ma. If fully heated (*bottom*), virtually all the grain ages are reset and represent the age of the last phase of cooling. The  $T_d$  (*shaded*) is time of deposition, which for all units are lower Cretaceous.

Intermediate peak ages and peak ages older than depositional age have limited utility because they have experienced an unknown amount of track shortening. We suspect that only the youngest two peak ages are of any general utility because partial annealing in the older suites cannot be ruled out. The youngest population (P1) in these samples is at 24–32 Ma (Late Oligocene), and it is defined by 10%–30% of the grains. Combined, the resulting

peak age is  $27 \pm 6$  Ma. The second-oldest population (P2), which is more significant in terms of the percentage of grains, falls between 57 and 68 Ma (mainly Paleocene) for those samples defined by more than 20% of the grains (table 2). A combined age for this population is 62.7 Ma ( $-7.8/+8.9$ ).

**Fully Reset Ages.** In these samples, zircons are fully reset to a common age, and the samples pass  $\chi^2$ . Within 2.5 km of the core of the Cordillera Huayhuash, there is only a narrow range of cooling ages from 10.9 to 15.6 Ma. Combined, they have a mean age of 11.6 Ma ( $-1.3/+1.4$ ; Middle Miocene).

**Single-Age Samples.** Granite and volcanic dikes have single uniform cooling ages. There are no granites mapped in the Huayhuash (Cobbing et al. 1997), but they are clearly present in the high topography because granitic boulders are common in glacial moraines. Their presence was recognized by Coney (1971), who suggested that they were covered by the glaciers. We suspect that they are located on the west flanks of North Rondoy. Either way, the granite samples were taken from an unknown granite intrusion but were collected from the crest of a young glacial moraine. Sample 03-17 has a cooling age of 10.9 Ma ( $-0.9/+1.0$ ), and sample 03-18 has a cooling age of 11.1 Ma ( $-0.9/+0.9$ ). They are identical in age to the young reset quartzite samples, and if all these samples are combined and run as a single sample, they have a mean age of  $11.0 \pm 1$  Ma (03-19, 03-22, 03-23, 03-18, 03-17).

Three different volcanic dikes were sampled, but only two yielded sufficient zircons for analysis. The first volcanic sample, 03-26, taken at an elevation of 4355 m, was a green hornblende-phyric dike that has a ZFT cooling age of 22.2 Ma ( $-3.8/+4.4$ ). The second, 03-27, is from an elevation of 4145 m and was a light-colored felsic dike with large beta quartz, feldspar, and mica phenocrysts. This sample has a cooling age of 6.2 Ma ( $-0.5/+0.6$ ).

**ZHe Ages.** We dated duplicate single-grain zircon samples from those that were entirely FT reset and two that were partially FT reset. Two reset samples from the central high topography were dated with ZHe. These samples are discussed from the central high area outward (figs. 6, 7). (1) A quartzite (03-19) has a ZFT cooling age of 10.9 Ma and ZHe cooling ages of 7.4 and 10.0 Ma. (2) A quartzite (03-22) has a ZFT cooling age of 12.7 Ma and a single successful ZHe cooling age of 7.0 Ma. (3) Farther away from the high topography, ZHe ages become older. Zircon from a quartzite (03-16) has ZHe cooling ages of 23.2 and 9.5 Ma (ZFT peak ages of ca. 27, 68, and 149 Ma from the same sample). (4) Finally, a quartzite (03-24) has a ZHe cool-

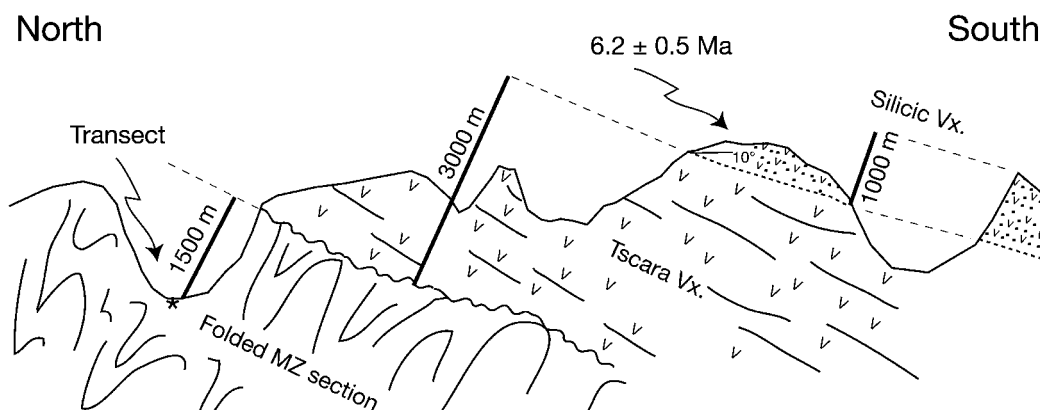


**Figure 9.** Sketch of relationships as outlined by Coney (1971) showing the southward tilting of the stratigraphic markers in the Cordillera Huayhuash. The most important is the southward tilt of the Puscanturpa Volcanics, which are inferred to be deposited on a nearly flat erosional surface. Our zircon fission track age at  $6.2 \pm 0.5$  Ma is on a quartz-phyric dike inferred to be a feeder to the lithologically identical Puscanturpa Volcanics. From these approximate thicknesses, we infer that burial by 5–5.5 km of rock is permissible for rocks in our transect (*asterisk*). See text for discussion.

ing age of 11.4 Ma. The ZFT ages are reset LRZ with populations of ca. 66 and 149 Ma.

**Thermal Maturity.** Although we have vitrinite reflectance data from only two samples in the middle of the transect, the results are illuminating. Both samples have a distribution of  $R_0$  values at ca. 1.7–1.8. Sample 25 has a bimodal distribution of  $R_0$  values and has maximum values of 4.7 as determined by biaxial negative reflectance cross plots (Kilby 1988). Optical continuity of reflectance appears to crosscut tectonic fabric, suggesting that peak temperatures occurred after deformation. Late Cretaceous to Early Tertiary thrusting caused burial, and coaly horizons may have acted as slip surfaces. Because sample 25 has a bimodal distribution of  $R_0$  values and because the lower value is common to both samples, it is likely that the heating to very high temperatures was extremely short lived (<1 m.yr.). We suspect this was associated with hot fluids because secondary mineralization is common and because the coal is unusually water rich for its rank. Together, the picture is one of a heterogeneous heating, and because the heating duration was probably very short, we are unable to compare these data to a standard calibration between  $R_0$  and temperature, but  $R_0$  of ca. 1.8 could correspond to temperatures of 150°–200°C if the duration was 1–25 m.yr. (Barker 1991).

### Implications

Our data reflect both end members of resetting for LRZs and HRZs. Reset samples in the core of the

Cordillera Huayhuash are an example of cooling from temperatures significantly higher than the effective closure temperature for ZFT. The zircons have limited radiation damage because they are from a Miocene pluton and thus have an effective closure temperatures of ca. 250°C (Brandon et al. 1998). Samples dated using ZHe should have a closure temperature of 160°–200°C (Reiners et al. 2002). Thus, the cooling age of a sample measured with ZHe should be lower than the cooling age of a sample measured with ZFT, but it may come close or overlap with thermal resetting of radiation damaged grains.

This second type of cooling age reflects heating to temperatures not significantly higher than the nominal ZFT closure temperature and is recorded by partial or full resetting of  $\alpha$ -damaged LRZs. This situation occurs when already cold rock (i.e., quartzites at high levels in the crust) with zircon grains of differing radiation damage are heated. In this case, LRZs anneal at lower temperatures than the less damaged, more retentive grains (Kasuya and Naeser 1988; Brandon et al. 1998). The LRZ grains could have been annealed at temperatures of ca. 180°–220°C, but the bounds of this temperature estimate are not well constrained (Laubacher and Naeser 1994; Brandon et al. 1998; Garver et al. 2002; Rahn et al. 2004). We recognize the following cooling intervals.

**Late Paleozoic.** Zircons from Cretaceous quartzites in the Huayhuash and the Cordillera Blanca appear to have a significant population of Permian cooling ages (242 and 299 Ma) from un-



**Figure 10.** Base camp for the upper part of our transect on the edge of Lago Jahuacocha (4200 m) looking east into the heart of the Cordillera Huayhuash. The prominent peak on the right horizon is Nevado Rondoy (5870 m). The reset zone is at the end of the lake and extends into the high peaks, which are composed of granites and quartzites that yield zircon fission track ages between 10.2 and 14.6 Ma. Note that local relief is in excess of 1500 m.

reset detrital samples. These are unreset ages that represent primary cooling ages in the original source region of the lower Cretaceous Chimu Formation. This period corresponds to a period of intense plutonism and volcanism recorded in the Permo-Triassic Mitu Formation, which is widespread in Peru (Dalmayrac et al. 1980). In the Eastern Cordillera of Peru, Laubacher and Naeser (1994) recognized multiple ZFT grain ages from granitic samples that also record this event.

*Paleocene.* The main age of thermal resetting of LRZs in the quartzites falls between 57 and 68 Ma (mainly Paleocene), with a combined mean age of ca. 63 Ma. An important question is whether these grains are only partly reset or fully reset. This interval follows structural imbrication and likely represents a period of postorogenic erosional exhumation inferred to have reduced the orogenic wedge to half its original imbricated thickness (Coney 1971). Deposition of continental red beds

occurred during this time. It is possible that this interval represents a thermal event associated with the intrusion of the Coastal Batholith, which was intruded in the Late Cretaceous. However, the nearest plutons of the Coastal Batholith are 30–50 km to the west, so it is likely that they had no direct thermal effect on rocks in the Huayhuash. This interval predates Incaic deformation, which occurred in the Eocene. We conclude that it is uncertain whether this cooling age is geologically meaningful and perhaps these are partly reset grains.

*Oligocene.* The young age of LRZ resetting in the quartzites falls between 24 and 32 Ma; combined, this young peak is 27 Ma (combined 03-13, 03-14, 03-16). This interval likely represents thermal resetting associated with the Tscara Volcanics and the correlative Calipuy Group. The volcanics rest unconformably on folded Jurassic and Cretaceous strata. These volcanic units represent a time



**Figure 11.** View to the south from near the transect line into the southern and western flanks of the Cordillera Huayhuash. The entire foreground is underlain by smooth-weathering folded Mesozoic metasediments. The person is standing at an elevation of about 4500 m. The peak in the background is underlain by the Tascara Volcanics (Oligo-Miocene) that rest unconformably on the folded Mesozoic section (fig. 7), and this surface is used to estimate the amount of erosion into the sequence. The unconformity, which dips away from this view, is defined by the prominent horizontal snowline across the middle of the mountain. Resistant rocks below the unconformity are near vertical feeder dikes, and all rocks in the foreground are folded Mesozoic sedimentary rocks.

of well-dated heating/mineralization from 33 to 15 Ma (Noble et al. 1999). Our ZFT age at 22 Ma on an intermediate feeder dike is likely part of this event. The rocks in the transect must have been at relatively shallow crustal levels before and during this event. In fact, the volcanic succession rests unconformably on an erosional surface cut into the Mesozoic section. Volcanism with widespread feeder dikes locally brought these near-surface rocks to temperatures sufficient to reset LRZs. Because most of the ZHe ages are younger than these ZFT ages, it is likely that temperatures during Late Oligocene volcanism were ca. 200°C. Higher temperatures would have reset more grains, and lower temperatures would not have been sufficient to reset ZHe ages.

*Middle to Late Miocene.* The core of the Huay-

huash has fully reset HRZ and ZHe ages of 7–15 Ma. Most of the HRZs from quartzites are reset to an age of ca.  $11 \pm 1$  Ma, and the cooling ages of the granitic rocks are the same. This common age represents a significant cooling period related to granitic emplacement and subsequent cooling. The ZHe ages are younger, and they decrease in age (7.5–11.4 Ma) away from the central core of the mountain range. The common age for the ZFT ages represents a single rapid cooling event, and younger ZHe ages are related to exhumation.

Miocene cooling followed intrusion and was partly driven by exhumation. In the Cordillera Blanca, erosion and normal faulting facilitated exhumation from the Late Miocene to the present. In the Cordillera Huayhuash, no significant normal faults are mapped (Cobbing et al. 1997), so it is



**Figure 12.** Photo looking west away from the Cordillera Huayhuash to the beginning of the transect in the deeply dissected Rio Pativilca drainage. This view is to the northwest to west, and the high peaks of the southern part of the Cordillera Blanca are just visible on the right horizon. There is a near concordance of summit elevations at about 4000 m in this area. Samples 13, 14, and 15 were taken from the drainage beyond the close ridge with near vertical folded Mesozoic quartzites. Relief in this drainage is about 2000 m.

likely that erosion has driven exhumation. To estimate exhumation rates, ZHe and ZFT ages and closure temperatures were evaluated. The two samples away from the core of the range have relatively slow apparent exhumation rates of ca. 15–50 m/m.yr. for the interval between 66 and 11 Ma. Our estimates suggest that these rocks cooled at rates of 12°–30°C/m.yr. between 10 and 7 Ma. Assuming a geothermal gradient between 25° and 50°C/km, this cooling would imply exhumation rates of 250–1300 m/m.yr. This time corresponds to the Vallé stage of development, the first phase and canyon incision driven ca. 2000 m of surface uplift of the Andes.

*Pliocene and Younger.* Reconstruction of the thickness of known stratigraphic units suggests that a maximum exhumation of ca. 5.0–5.5 km has occurred in the upper reaches of the Rio Achin since 6 Ma (fig. 9; Coney 1971). The Miocene Pus-

canturpa Volcanics have a maximum exposed thickness of 1000 m and sit unconformably on top of the Calipuy Volcanics, which have a thickness of ca. 3000 m. Both of these units are exposed to the south of our study area, and the deeper levels of exposure to the north are due to a slight (10°) tilt of rocks to the south. There is considerable relief in the area (fig. 10). The elevation of the sub-Tascara unconformity along the transect would allow an additional 1000–1500 m of deformed rock, which includes folded Mesozoic rocks (figs. 11, 12; Coney 1971). Thus, the samples dated in the upper Achin could have had a maximum of 5.0–5.5 km of overlying rock that is now being removed by erosion. Because a minimum of 230°–250°C is required to fully reset HRZs over time periods of 1–5 m.yr., the geothermal gradient must have been equal to or greater than 45°–55°C/km. This high gradient could have resulted from Miocene plutonism. Recall that

our estimate of paleotemperatures associated with the thermal resetting of the ZHe ages (but not LRZ FT ages) suggested maximum temperatures of ca. 180°–200°C in the Late Miocene, before cover by the Puscanturpa Volcanics (6–7 Ma). At this time, there was probably a maximum cover of 4–4.5 km of rock above the transect line (pre-Puscanturpa), which would imply a geothermal gradient of ca. 40°–50°C/km. The important point here is that with the known rock column, the paleogeothermal gradient must have been rather high in the Miocene. We suspect that this was the case in a large area of this part of the Andes. This interval corresponds to widespread mineralization in addition to plutonism, so thermochronological studies aimed at understanding Andean uplift and exhumation must take this event into consideration.

The Cordillera Blanca to the north also has high topography and relief in excess of 3 km. This range is also underlain by Miocene plutonic rocks that were deeply exhumed from 9 km since intrusion. Much of the exhumation is attributed to movement on the Cordillera Blanca normal fault (McNulty and Farber 2002), and exhumation has been rapid and ongoing since ca. 5.5 Ma (Garver et al. 2003; Perry 2004; Perry and Garver 2004). Like the Huayhuash Range, the preexhumation events in the Cordillera Blanca area are marked by silicic volcanism. Here, silicic volcanics of the Yungay Formation, which is preserved today in the hanging wall of the Cordillera Blanca normal fault, erupted from 7.15 to 6.4 Ma (Wise and Noble 2002; Giovanni et al. 2003; Perry 2004). The youngest reliable ages are on volcanics interbedded with strata of the hanging wall basin that records erosional exhumation of the Cordillera Blanca (i.e., Bonnot et al. 1988). Thus, these rocks, which are just to the north along the crest of the Andes, experienced rapid and deep exhumation since ca. 6 Ma, and the latest phase of exhumation corresponds to the Cañon stage of erosion driven by the second phase of surface uplift in this part of the Andes.

The latest phase of exhumation in both the Huayhuash and the Blanca apparently has occurred since 5–6 Ma. This latest phase of exhumation and canyon incision is ongoing and corresponds to the Cañon stage of erosion widely recognized throughout this part of the Andes.

### Conclusions

The main phase of cooling occurred at 11 Ma along the highest topography in the central part of the Cordillera Huayhuash. Other rocks along the traverse are variably reset and probably reflect several

earlier cooling events. The main phase rocks were cooled by two processes. In the Late Miocene, the area was intruded by granitic plutons along what is now the main drainage divide (Coney 1971). The average age of cooling of reset rocks through ZFT closure is  $11.4 \pm 1$  Ma, and this cooling likely followed intrusion of granitic rocks, which are today barely exposed in the high topography. After the intrusion, the rocks were exhumed as the uplift of the Cordillera Huayhuash progressed. Dissection of the uplifted block was caused by the incising rivers (especially Rio Pativilca; Coney 1971). As incision removed significant rock from the western flanks of the Andes, isostatic adjustment would have driven further uplift with peak elevations of almost double the original uplifted elevation (Molnar and England 1990). In this case, an original uplift of this part of the Andes to an elevation of ca. 3600 m, once fully incised, would have summit elevations as high as ca. 6500 m, and canyons incised to about the original elevation. Both aspects are seen in this area (figs. 2, 3). As outlined previously, it is likely that uplift of the Andes in this specific area was largely accomplished by 5–6 Ma, and the incision and subsequent feedback uplift has occurred since.

A recent hypothesis suggests that the overall uplift in the Andes has been driven by lack of sediment in the nearby trench causing higher than normal shear stresses (Lamb and Davis 2003). This hypothesis suggests that sediment starvation of the trench has caused increased shear stress at the plate interface and notes that an anomalous segment in the Andes is in the Cordillera Blanca area, which includes the Cordillera Huayhuash. Here, there is a lower than anticipated calculated shear stress, which suggests excess lubrication of the subduction zone, which can be caused by a thick sediment blanket in the trench. We have concluded that erosional exhumation of the western flanks of the Cordillera Huayhuash (Pacific draining) has been accomplished since the Late Miocene. As such, one possible reason for this discrepancy in calculated shear stress along the plate boundary is that this segment has seen profound erosion and sediment deposition in the trench in the last 5–6 m.yr.

### ACKNOWLEDGMENTS

We would like to thank S. Nicolescu for help with (U-Th)/He analyses. S. Reese (Oregon State University) expedited irradiation of the FT samples, which was funded under the U.S. Department of Energy Reactor Use Sharing program. J. Newman at Newman Energy Research (Christchurch, New

Zealand) did the vitrinite work and helped with the interpretation of the vitrinite reflectance data. Ideas in this article emerged from fruitful discussions with J. Wise, M. T. Brandon, C. Naeser, J. Vance, B. C. D. Riley, M. Bernet, and D. T. Rodbell. A. Ames facilitated logistics in Peru, and his help is much appreciated. Field studies were funded by the Union College Internal Education fund (S. E. Perry,

L. J. Walker) and Union College Faculty Research Fund (J. I. Garver). J. I. Garver acknowledges an Erskine Fellowship from the University of Canterbury (New Zealand) through the Department of Geological Sciences, which supported him during the writing of this article. This article has benefited from thoughtful and constructive reviews by C. W. Naeser and S. N. Thomson.

#### REFERENCES CITED

- Allmendinger, R. W.; Jordan, T. E.; Kay, S. M.; and Isacks, B. L. 1997. The evolution of the Altiplano-Puna Plateau of the central Andes. *Annu. Rev. Earth Planet. Sci.* 25:139–174.
- Anders, M. H.; Gregory-Wodzicki, K. M.; and Spiegelman, M. 2002. A critical evaluation of late Tertiary accelerated uplift rates for the Eastern Cordillera, central Andes of Bolivia. *J. Geol.* 110:89–100.
- Barker, C. E. 1991. Implications for organic maturation studies of evidence for a geologically rapid increase and stabilization of vitrinite reflectance at peak temperature: Cerro Prieto Geothermal System, Mexico. *Am. Assoc. Pet. Geol. Bull.* 75:1852–1863.
- Benjamin, M. T.; Johnson, N. M.; and Naeser, C. W. 1987. Recent rapid uplift in the Bolivian Andes: evidence from fission-track dating. *Geology* 15:680–683.
- Bernet, M. 2002. Exhuming the Alps through time: clues from detrital zircon fission-track ages. PhD thesis, Yale University, New Haven, CT.
- Bonnot, D.; Sébrier, M.; and Mercier, J. 1988. Evolution géodynamique Pliocénaire du bassin intra-cordillerien du Callejon de Huaylas et de la Cordillere Blanche, Perou. *Geodynamique* 3:57–83.
- Bowman, I. 1906. The Andes of southern Perú, Geological reconnaissance along the 73 meridian. *Am. Geogr. Soc. Spec. Publ.* 1, 336 p.
- Brandon, M. T. 1996. Probability density plot for fission-track ages of detrital zircon grain-age samples. *Radiat. Meas.* 26:663–676.
- Brandon, M. T.; Roden-Tice, M. R.; and Garver, J. I. 1998. Late Cenozoic exhumation of the Cascadia accretionary wedge in the Olympic Mountains, northwest Washington State. *Geol. Soc. Am. Bull.* 100:985–1009.
- Brandon, M. T., and Vance, J. A. 1992. Fission-track ages of detrital zircon grains: implications for the tectonic evolution of the Cenozoic Olympic subduction complex. *Am. J. Sci.* 292:565–636.
- Brix, M. R.; Stöckhert, B.; Seidel, E.; Theye, T.; Thomson, S. N.; and Küster, M. 2002. Thermobarometric data from a fossil zircon partial annealing zone in high pressure–low temperature rocks of eastern and central Crete. *Tectonophysics* 349:309–326.
- Carter, A. 1990. The thermal history and annealing affects of zircons from the Ordovician of North Wales. *Nucl. Tracks Radiat. Meas.* 17:309–313.
- Chakoumakos, B. C.; Murakami, T.; Lumpkin, G. R.; and Ewing, R. C. 1987. Alpha-decay-induced fracturing in zircon: the transition from the crystalline to the metamict state. *Science* 236:1556–1559.
- Cobbing, E. J.; Pitcher, W. S.; Wilson, J. J.; Baldock, W. P.; McCourt, W.; and Snelling, N. J. 1981. The geology of the western Cordillera of northern Peru. *Overseas Mem. Inst. Geol. Sci. Lond. Mem.* 5, 143 p.
- Cobbing, E. J.; Saucuez, A. F.; Martinez, V. W.; and Zarate, O. H. 1997. *Geologica de los Cuadrangulos de Huaraz, Recuay, La Union, Chiquian y Yanahuanca*; hojas 20-h, 20-I, 21-I, 21-j. *Bol. Inst. Geol. Minero Metalurgico Perú, Ser. A, Carta Geologica Nacional Rep.* 76, 286 p.
- Coltorti, M., and Ollier, C. D. 1999. The significance of high planation surface in the Andes of Ecuador. *In* Smith, B. J.; Whalley, W. B.; and Warke, P. A., eds. *Uplift, erosion and stability: perspectives on long-term landscape development.* *Geol. Soc. Lond. Spec. Publ.* 162:239–253.
- Coney, P. J. 1971. Structural evolution of the Cordillera Huayhuash, Andes of Peru. *Geol. Soc. Am. Bull.* 82: 1863–1884.
- Coyle, D. A., and Wagner, G. A. 1996. Fission-track dating of zircon and titanite from the 9101 m deep KTB: observed fundamentals of track stability and thermal history reconstruction. *Ghent, International Workshop on Fission Track Dating*, p. 22.
- Dalmayrac, B.; Laubacher, G.; and Marocco, R. 1980. Carctères généraux de l'évolution géologique des Andes Péruviennes. *Travaux et Documents de l'ORSTOM* 122. Paris, Office de la Recherche Scientifique et Technique Outre-Mer, 501 p.
- Ellsworth, S.; Navrotsky, A.; and Ewing, R. C. 1994. Energetics of radiation damage in natural zircon (ZrSiO<sub>4</sub>). *Phys. Chem. Miner.* 21:140–149.
- England, P., and Molnar, P. 1990. Surface uplift, uplift of rocks, and exhumation of rocks. *Geology* 18:1173–1177.
- Ewing, R. C. 1995. Radiation effects in nuclear waste forms for high-level radioactive waste. *Prog. Nucl. Energy* 29:63–127.
- Farley, K. A. 2002. (U-Th)/He dating: techniques, calibrations, and applications. *In* Porcelli, D.; Ballentine, C. J.; and Wieler, R., eds. *Noble gases in geochemistry and cosmochemistry.* *Rev. Mineral. Geochem.* 47: 819–843.
- Farley, K. A.; Wolf, R. A.; and Silver, L. T. 1996. The

- effects of long alpha-stopping distances on (U-Th)/He ages. *Geochim. Cosmochim. Acta* 60:4223–4229.
- Garver, J. I., and Bartholomew, A. 2001. Partial resetting of fission tracks in detrital zircon: dating low-temperature events in the Hudson Valley (NY). *Geol. Soc. Am. Abstr. Program* 33:82.
- Garver, J. I.; Brandon, M. T.; Bernet, M.; Brewer, I.; Soloviev, A. V.; Kamp, P. J. J.; and Meyer, N. 2000. Practical consideration for using detrital zircon fission track thermochronology for provenance, exhumation studies, and dating sediments. 9th International Conference on Fission-Track Dating and Thermochronology. *Geol. Soc. Aust. Abstr.* 58:109–111.
- Garver, J. I., and Kamp, P. J. J. 2002. Integration of zircon color and zircon fission track zonation patterns in orogenic belts: application of the Southern Alps, New Zealand. *Tectonophysics* 349:203–219.
- Garver, J. I.; Riley, B. C. D.; and Wang, G. 2002. Partial resetting of fission tracks in detrital zircon. European Fission-Track Conference, Cadiz, Spain. *Geotemas* 4: 73–75.
- Garver, J. I.; Schiffman, C. R.; and Perry, S. E. 2003. Rapid tectonic exhumation of the Cordillera Blanca. *Geol. Soc. Am. Abstr. Program* 35:429.
- Giovanni, M. K.; Horton, B. K.; McNulty, B.; and Grove, M. 2003. Evolution of the Cordillera Blanca Normal Fault, Central Peruvian Andes: evidence from Basin Analysis and  $^{40}\text{Ar}/^{39}\text{Ar}$  thermochronology. *EOS: Trans. Am. Geophys. Union* 84:46.
- Green, P. F.; Hegarty, K. A.; Duddy, I. R.; Foland, S. S.; and Gorbachev, V. 1996. Geological constraints on fission track annealing in zircon. Ghent, International Workshop on Fission-Track Dating, p. 44
- Gregory-Wodzicki, K. M. 2000. Uplift history of the central and northern Andes: a review. *Geol. Soc. Am. Bull.* 112:1091–1105.
- Kasuya, M., and Naeser, C. W. 1988. The effect of  $\alpha$ -damage on fission-track annealing in zircon. *Nucl. Tracks Radiat. Meas.* 14:477–480.
- Kennan, L. 2000. Large-scale geomorphology of the Andes: interrelationships of tectonics, magmatism and climate. In Summerfield, M. A., ed. *Geomorphology and global tectonics*. New York, Wiley, p. 167–199.
- Kilby, W. E. 1988. Recognition of vitrinite with non-uniaxial negative reflectance characteristics. *Int. J. Coal Geol.* 9:267–285.
- Lamb, S., and Davis, P. 2003. Cenozoic climate change as a possible cause for the rise of the Andes. *Nature* 425:792–797.
- Laubacher, G., and Naeser, C. W. 1994. Fission-track dating of granitic rocks from the Eastern Cordillera of Peru, evidence for Late Jurassic and Cenozoic cooling. *J. Geol. Soc. Lond.* 151:473–483.
- McNulty, B., and Farber, D. 2002. Active detachment faulting above the Peruvian flat slab. *Geology* 30:567–570.
- McNulty, B. A.; Farber, D. L.; Wallace, G. S.; Lopez, R.; and Palacios, O. 1998. Role of plate kinematics and plate-slip-vector partitioning in continental magmatic arcs: evidence from the Cordillera Blanca, Peru. *Geology* 26:827–830.
- Megard, F. 1987. Structure and evolution of the Peruvian Andes. In Schaer, J. P., and Rogers, J., eds. *Anatomy and mountain ranges*. Princeton, NJ, Princeton University Press, p. 179–210.
- Molnar, P., and England, P. 1990. Late Cenozoic uplift of mountain ranges and global climate change: chicken or egg? *Nature* 346:29–34.
- Montgomery, D. R.; Balco, G.; and Willett, S. D. 2001. Climate, tectonics, and the morphology of the Andes. *Geology* 29:579–582.
- Myers, J. S. 1980. Geologia de los Cuadrángulos de Huaramey y Huayllapampa (hojas: 21-j y 21-h). Lima, Inst. Geol. Minero Metalurgico Bol. 33, 154 p.
- Naeser, C. W. 1979. Fission-track dating and geologic annealing of fission-tracks. In Jager, E., and Hunziker, J. C., eds. *Lectures in isotope geology*. Heidelberg, Springer, p. 154–169.
- Nasdala, L.; Reiners, P. W.; Garver, J. I.; Kennedy, A. K.; Stern, R. A.; Balan, E.; and Wirth, R. 2004. Incomplete retention of radiation damage in zircon from Sri Lanka. *Am. Mineral.* 89:219–231.
- Noble, D. C.; Wise, J. M.; Vidal, C. E.; and Heizler, M. T. 1999. Age and deformational history of the “Calipuy Group” in the Cordillera Negra, Northern Peru. *Aniversario Soc. Geol. Peru* 5:219–226.
- Perry, S. E. 2004. Thermochronologic evolution of the Cordillera Blanca, Northern Peru, based on zircon and apatite fission-track and U+Th/He dating. BS thesis, Union College, Schenectady, NY.
- Perry, S. E., and Garver, J. I. 2004. Onset of tectonic exhumation of the Cordillera Blanca, Northern Perú, based on fission-track and U+Th/He dating of zircon. *Geol. Soc. Am. Abstr. Program* 36:92.
- Rahn, M. K.; Brandon, M. T.; Batt, G. E.; and Garver, J. I. 2004. A zero model for fission-track annealing in zircon. *Am. Mineral.* 89:473–484.
- Reiners, P. W.; Farley, K. A.; and Hickes, H. J. 2002. He diffusion and (U-Th)/He thermochronometry of zircon: initial results from Fish Canyon Tuff and Gold Butte. *Tectonophysics* 349:247–308.
- Reiners, P. W.; Spell, T. L.; Nicolescu, S.; and Zanetti, K. A. 2004. Zircon (U-Th)/He thermochronometry: He diffusion and intercalibration with  $^{40}\text{Ar}/^{39}\text{Ar}$  dating. *Geochim. Cosochim. Acta* 68:1857–1887.
- Reiners, P. W.; Zhou, Z.; Ehlers, T. A.; Xu, C.; Brandon, M. T.; Donelick, R. A.; and Nicolescu, S. 2003. Post-orogenic evolution of the Dabie Shan, eastern China, from (U-Th)/He and fission-track dating. *Am. J. Sci.* 303:489–518.
- Riley, B. C. D. 2003. Laramide exhumation and heating in southeastern Arizona: low-temperature thermal history and implications for zircon fission-track systematics. PhD dissertation, University of Texas at Austin.
- Riley, B. C. D., and Garver, J. I. 2002. Preferential thermal resetting of fission tracks in radiation-damaged detrital zircon grains: case study from the Laramide of Arizona. *Geol. Soc. Am. Abstr. Program* 34:485.

- Ring, U.; Brandon, M. T.; Willett, S. D.; and Lister, G. S. 1999. Exhumation processes. *In* Ring, U.; Brandon, M. T.; Lister, G. S.; and Willet, S. D., eds. Exhumation processes: normal faulting, ductile flow and erosion. Geol. Soc. Lond. Spec. Publ. 154:1–27.
- Rodbell, D. T., and Seltzer, G. O. 2000. Rapid ice margin fluctuations during the Younger Dryas in the Tropical Andes. *Quat. Res.* 54:328–337.
- Schiffman, C. R. 2003. The evolution of the Seismogenic Cordillera Blanca normal fault, Peru, and its relationship to long-term exhumation rates, based on zircon fission-track analysis. BS thesis, Union College, Schenectady, NY.
- Sébrier, M.; Lavenu, A.; Fornari, M.; and Soulas, J.-P. 1988. Tectonics and uplift in central Andes (Perú, Bolivia, and northern Chile) from Eocene to present. *Geodynamique* 3:85–106.
- Seward, D., and Rhodes, D. A. 1986. A clustering technique for fission track dating of fully to partially annealed mineral and other non-unique populations. *Nucl. Tracks Radiat. Meas.* 11:259–268.
- Tagami, T.; Carter, A.; and Hurford, A. J. 1996. Natural long term annealing of the zircon fission-track system in Vienna Basin deep borehole samples: constraints upon the partial annealing zone and closure temperature. *Chem. Geol.* 130:147–157.
- Tagami, T.; Galbraith, R. F.; Yamada, R.; and Laslett, G. M. 1998. Revised annealing kinetics of fission tracks in zircon and geological implications. *In* van den Haute, P., and de Corte, F., eds. Advances in fission-track geochronology. Norwell, MA, Kluwer Academic, p. 99–112.
- Thomson, S. N. 2002. Late Cenozoic geomorphic and tectonic evolution of the Patagonian Andes between latitudes 42°S and 46°S: an appraisal based on fission-track results from the transpressional intra-arc Liquiñe-Ofqui fault zone. *Geol. Soc. Am. Bull.* 114: 1159–1173.
- Tosdal, R. M.; Clark, A. H.; and Farrar, E. 1984. Cenozoic polyphase landscape and tectonic evolution of the Cordillera Occidental, southernmost Perú. *Geol. Soc. Am. Bull.* 95:1318–1332.
- Wilson, J. J.; Reyes, L.; and Garayer, J. 1967. Geología de los cuadrangulos de Mollebamba, Tayamba, Huaylas, Pomabamba, Caruaz y Huari. Lima, Bol. Serv. Geol. Mina. 16, 95 p.
- . 1995. Geología de los Cuadrangulos de Pallasca, Tayabamba, Corongo, Pomabamba, Carhuaz, Y Huari. Lima, Inst. Geol. Sci.
- Wise, J., and Noble, D. 2002. Scientific comment on the nature and origin of the Cordillera Blanca normal fault. *Bol. Soc. Geol. Peru* 94:107–108.